Fuel 97 (2012) 245–252

Contents lists available at SciVerse ScienceDirect

Fuel

journal homepage: www.elsevier.com/locate/fuel

Effect of nature of ceria support in CuO/CeO_2 catalyst for PROX-CO reaction

Cristhiane Guimarães Maciel [a,*], Tatiana de Freitas Silva [a], Marcelo Iuki Hirooka [a], Mohamed Naceur Belgacem [b], Jose Mansur Assaf [a]

[a] Universidade Federal de São Carlos, Departamento de Engenharia Química, Via Washington Luiz, Km 235, CEP 13565-905, São Carlos, SP, Brazil
[b] Grenoble Institute of Technology (INP Grenoble-PAGORA), 461 rue de la Papeterie, BP 65, F-38402 St. Martin d'Heres Cedex, France

ARTICLE INFO

Article history:
Received 28 April 2011
Received in revised form 30 January 2012
Accepted 2 February 2012
Available online 22 February 2012

Keywords:
Ceria
Hydrothermal
Precipitation

ABSTRACT

In order to understand the effect of CeO_2 on the preferential CO oxidation reaction (PROX-CO), the support cerium oxide was prepared by hydrothermal (CeO_2-HT) and precipitation (CeO_2-PP) methods. The catalyst supported on CeO_2-HT exhibited higher activity than CuO/CeO_2-PP. Characterization revealed that CuO was better dispersed on the CuO/CeO_2-HT surface favoring the PROX-CO reaction, compared to CuO/CeO_2-PP. Also, the nature of ceria was important for enhancing the metal-support interaction, which affects the catalytic activity. The CuO/CeO_2-HT catalyst was less sensitive to presence of CO_2 and H_2O, remaining stable in a 24 h run.

1. Introduction

Cerium dioxide (ceria, CeO_2) and ceria based materials are promising materials for a number of applications and as one of the most important components in high-performance three-way catalyst (TWC) for its capability of enhancing the removal of CO, NO_x and hydrocarbons, working as an oxygen storing component. Also, ceria is widely employed as the support or additive in catalysts for oxidation reactions because of its high oxygen storage capacity and redox activity [1–5].

Additionally, ceria has become an important material in several fields of modern technology and different functions are widely related to ceria existing in two oxidation states, trivalent and tetravalent, and the charge transfer can be represented by Ce^{+4}–O^2 [5]. The ability of ceria to undergo rapid redox cycles is responsible for its oxygen storage capacity (OSC). One important aspect that must be carefully observed is the loss of oxygen storage capacity due to the sintering of CeO_2 particles and grain growth at higher temperatures [4].

Great attention is being paid to the production of nanocrystalline ceria powders, to achieve better catalytic activity, improved redox properties and a higher ionic conductivity in comparison with those of microcrystalline CeO_2 [5]. The removal of oxygen from CeO_2 at high temperatures and under a reducing atmosphere leads to the production of an oxygen-deficient nonstoichiometric CeO_{2-y} phase with $0 < y < 0.5$. This phase retains the same fluorite crystal structure as CeO_2, facilitating the rapid and complete refilling of every oxygen vacancy upon exposure of CeO_{2-y} to oxygen, with recovery of CeO_2 [3,4,6].

According to Wootsch et al., the CO oxidation in a reducing atmosphere could be analogous to the three-way catalysis (TWC) in the case of automotive exhaust post treatment [7]. Thus, ceria is extensively used like support on CO preferential oxidation (PROX-CO) and when combined with copper, excellent results of activity and selectivity have been found.

The preferential CO oxidation reaction (PROX-CO) involves the oxidation of CO to CO_2 without the simultaneous oxidation of H_2 to H_2O (Eqs. (1) and (2) respectively). Therefore, the catalyst for PROX-CO reaction must be active and selective, avoiding oxidation of H_2 significant amounts. The main goal of PROX-CO reaction is the purification of the H_2, reducing the CO concentration to 10–100 ppm, a level tolerated by the Pt electrocatalyst in the proton exchange membrane fuel cell (PEMFC) [1–10].

$$CO + \frac{1}{2}O_2 \leftrightarrow CO_2 \quad (1)$$

$$H_2 + \frac{1}{2}O_2 \leftrightarrow H_2O \quad (2)$$

Ceria has an important role in the metal/support interactions induced by the establishment of close contact between both components, what strongly affects their redox and, in consequence, catalytic properties. For systems containing copper and ceria, the establishment of intimate contacts between both components is thought to be of crucial importance in explaining the

* Corresponding author. Fax: +55 16 3351 8266.
E-mail address: mansur@ufscar.br (C.G. Maciel).

0016-2361
doi:10.1016/j.fuel.2012.02.004

remarkably high activities exhibited by CuO/CeO_2 catalyst for carbon monoxide oxidation. The promoting effect of ceria was proposed to be due to both change in redox state capacity and bifunctional promotion. Thus, a synergistic reaction model to explain the enhanced catalytic activity shown by Cu–Ce oxides has been proposed, in which Cu^+ species, stabilized by interactions between copper oxide, clusters and cerium oxide provide surface sites for CO adsorption, while the cerium oxide provides oxygen vacancies [8]. Furthermore, CuO and CeO_2 could easily adsorb CO. As consequence, this catalyst exhibited a high activity/selectivity for the low temperature CO oxidation. Additionally, that redox processes underwent upon the CO oxidation involved in the reduction and the oxidation of both the copper and the ceria phases. The addition of copper in the load enhances the redox behavior, the oxygen storage capacity and the thermal stability of ceria [9,10].

Several methods have been developed to synthesize CeO_2 powders with different results. In this work, a comparative study with CuO/CeO_2 catalyst for CO preferential oxidation has been done with CeO_2 prepared by the conventional precipitation process and a by hydrothermal method.

2. Experimental

2.1. Catalysts preparation

Ceria powder was prepared by precipitation and hydrothermal methods. For precipitation, the solid obtained was named CeO_2-PP. For this, $Ce(NO_3)_2.6H_2O$ was the precursor salt and the preparation procedure consisted in mixing the aqueous nitrate and NH_4OH (1 M) solutions under heating at 60 °C and stirring for 4 h. The resulting precipitate was filtered and washed with deionized water. Finally, the solid was dried at 60 °C for 12 h and calcined in synthetic air atmosphere (80 cm^3 min^{-1}) for 4 h. A heating rate of 1 °C min^{-1} was used in the calcination step. Catalyst prepared with CeO_2-PP was named CuO/CeO_2-PP (5 wt% copper). Ceria prepared by hydrothermal method [11,12] was named CeO_2-HT and used as support for CuO/CeO_2-HT catalyst (5 wt% copper). The catalysts CuO/CeO_2-PP and CuO/CeO_2-HT were prepared by the deposition–precipitation method where $Cu(NO_3)_2.3H_2O$ was employed as precursor. Aqueous solution containing urea enough to get to a molar ratio copper:urea of 1:3 was added to mixture. The whole solution was heated at 80 °C until complete solvent vaporization. The final solid was dried at 60 °C for 24 h. All the catalysts were calcined at 500 °C for 4 h under air flow of 80 cm^3 min^{-1} and at heating rate of 1 °C min^{-1}.

2.2. Catalyst characterization

X-ray diffraction (XRD) patterns of the powder samples were obtained with a Rigaku Multiflex diffractometer with Cu Kα radiation. The X-ray spectra were compared with the patterns in JCPDS to identify the crystalline phases. The average dimension of the crystallites was determined by Scherreŕs equation.

Surface area was measured by the N_2-adsorption – BET method in a Quantachrome Nova 1200 surface analyzer.

Information about the reducibility of the oxide species was obtained by temperature-programmed reduction (TPR) in Micromeritics Pulse Chemisorb 2705 equipment, using a heating rate of 10 °C min^{-1} from room temperature up to 800 °C. The reducing gas used was a 5% H_2/N_2 flowing mixture at 30 mL min^{-1}.

Fourier transformed infrared (FTIR, PerkinElmer Instruments – Paragon 1000) spectra of the catalyst were collected at room temperature using KBr pellet samples.

The morphology and the crystal shape of the prepared catalysts particles were examined by transmission electron microscopy (TEM) and gun-scanning electron microscopy (FEGSEM) with a Philips CM120 transmission electron microscope operated at 200 kV and a Zeiss Ultra-55 field emission gun-scanning electron microscope (FEGSEM).

X-ray photoelectron spectroscopy (XPS) experiments were carried out with an XR3E2 apparatus (Vacuum Generators, UK) equipped with a monochromated Mg KR X-ray source (1253.6 eV) and operating at 15 kV under a current of 20 mA to determine the surface composition of the catalysts.

Elemental analysis was carried out at the Laboratoire Centrale d'Analyses de Vernaison to determine the bulk composition of the catalysts. The technique was based on atomic absorption of the investigated elements.

2.3. Catalytic activity measurements

PROX-CO reactions were performed in a glass tubular fixed-bed reactor (5 mm i.d.) operating under atmospheric pressure. That reaction was named as ideal PROX-CO. Samples (400 mg) were reduced *in situ* with pure H_2 at 300 °C for 2 h, under flow of 30 cm^3 min^{-1}. Gases mixture of 4% CO, 2% O_2, 50% H_2 and N_2 was prepared by adjusting the rates of flow mass controllers (MKS Instruments 247, with four channels). The tests were performed by decreasing the temperature from 300 °C to 100 °C in steps of 50 °C. The reactor temperature was monitored by a thermocouple and controlled by a Flyever FE50RP temperature controller. Gas chromatography (GC) analyses were performed in triplicate at each temperature step, in order to allow the reaction system to stabilize. The analyses were performed in-line in a VARIAN 3800 chromatograph equipped with thermal conductivity detectors (TCDs). The effluent gases were split into two streams, the first one using He as a carrier gas and eluted on a 13× column in series with a Porapak column; the second one used N_2 as carrier gas, eluted on a molecular sieve 13× column. Each streams was monitored at the outlet with a TCD.

The effects of H_2O and CO_2 in the feed stream were evaluated by adding of 10 mol% H_2O and 15 mol% CO_2 to the feed gas in order to simulate the effluent's real stream composition in the steam reforming reactor. That reaction was called real PROX-CO. Activation conditions identical to the used in ideal PROX-CO reaction were utilized in that test. Long-term stability test (24 h) was realized with real PROX-CO conditions at 150 °C.

The reactor effluents were analyzed by using an in-line chromatograph (GC 3800-VARIAN), with two thermal conductivity detectors, Porapak N and 13× molecular sieves packed columns.

The conversions of CO (X_{CO}) and O_2 (X_{O2}), as well as the selectivity of CO oxidation (S_{CO}) in hydrogen excess, were calculated as follows:

$$X_{(CO)}\% = \frac{[CO]_{in} - [CO]_{out}}{[CO]_{in}} \times 100$$

$$X_{(O_2)}\% = \frac{[O_2]_{in} - [O_2]_{out}}{[O_2]_{in}} \times 100$$

$$S_{(CO)}\% = \frac{0.5([CO]_{in} - [CO]_{out})}{[O_2]_{in} - [O_2]_{out}} \times 100$$

3. Results and discussion

Reducibility analyses of the oxide species are illustrated in Fig. 1. The reduction profiles of the CeO_2-HT and CeO_2-PP supports are similar, with two reduction shoulders at low temperatures and

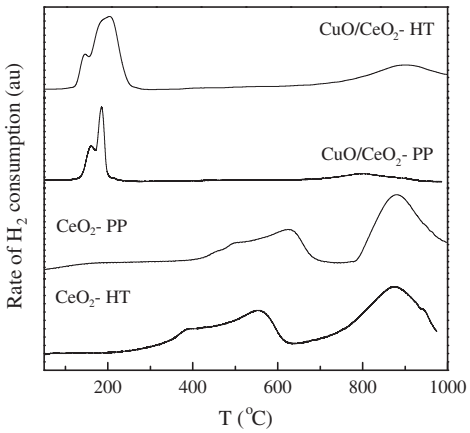

Fig. 1. H_2-TPR profiles of CeO_2-HT, CeO_2-PP and CuO/CeO_2 catalysts.

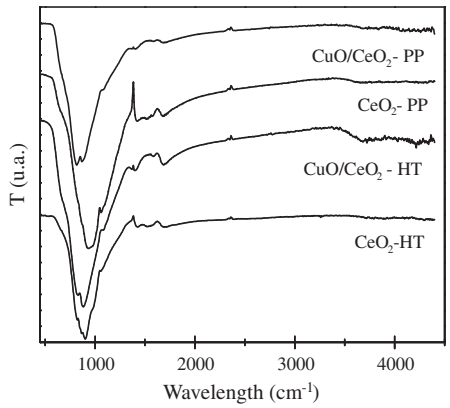

Fig. 2. FTIR analysis of CeO_2-HT, CeO_2-PP and CuO/CeO_2 catalysts.

an intense peak at high temperatures. However, the reduction temperatures of the two supports are not the same. According to Yee et al., surface reduction of CeO_2 under H_2 occurs at 473 °C and ceria bulk reduction occurs at temperatures above 923 °C [6]. The reduction of ceria prepared by the hydrothermal method started at 389 °C, while the ceria prepared by precipitation shows the first shoulder at 500 °C. The same tendency is observed again for the second reduction shoulder and the high temperature peak: in CeO_2-HT, these reductions take place between 558 and 874 °C, while in CeO_2-PP they occur between 623 and 880 °C. The shoulders at lower temperatures are related to the reduction of ceria surface oxygen, while the high temperature peak is related to bulk ceria reduction.

The H_2-TPR profiles of copper-containing catalysts samples show two peaks at different temperatures under 200 °C and one at a temperature higher than 800 °C. The lower temperatures peaks are due to the reduction of the superficial CuO associated with ceria, of small-sized particles, and to the reduction of bulk CuO, larger than the superficial one. The high temperature peak refers to ceria bulk. Similar results were found by several authors in the literature. The identification of the H_2-TPR peaks can be elucidated in combination with XRD analysis and *in situ* XRD experiments [13–18]. As both catalysts were prepared under the same conditions with the same CuO loading, the differences in reduction temperature can be attributed to the support effect. In the CuO/CeO_2-HT, the CuO reduction is favored when compared to the precipitated catalyst (peaks at 139 and 185 °C in CeO_2-HT and at 158 and 194 °C in CuO/CeO_2-PP). Despite the ceria reduction temperature is lower for the CuO/CeO_2-PP catalyst, the reduction degree is smaller, while for the CuO/CeO_2-HT this reduction is more intense. In other words, the reduction of ceria in CuO/CeO_2-HT is more favored that in CuO/CeO_2-PP.

Both copper species are active for CO oxidation, but the species reduced at low temperature are more reactive than the copper at smaller dispersion state. These observed differences, in both the cerium and copper oxides are important for understanding the catalytic performance of each solid [19–21].

Fourier transformed infrared spectra for supports and catalysts are shown in Fig. 2. These spectra are similar, indicating that the IR absorbing species are the same in all four materials. Small band displacements are observed, in which different precursor salts were used. The bands shown at 1700 cm^{-1} correspond to the O–H bond's vibration, υ(OH) [22–24]. These bands are more intense for CeO_2-PP, CeO_2-HT and CuO/CeO_2-HT, indicating that these species are more susceptible to hydration. The bands centered at 1043 and 883 cm^{-1} may be attributed to υC–O and $\delta - CO_3^{2-}$, respectively, and the bands found at 2360 cm^{-1} are due to the CO_2 absorbed from the atmospheric [22,23]. No absorption bands related to nitrates were found, indicating that the preparation conditions and heat treatment were effective, resulting in the formation of catalysts containing only CuO and/or CeO_2.

Fig. 3 shows the XRD patterns of supports and catalysts: the diffraction peaks of both supports and supported catalysts are characteristic of ceria, with a fluorite structure. No Cu^0, Cu_2O or CuO peaks were found, what can be explained by CuO being amorphous or incorporated into the CeO_2 lattice with small size particles or being so well dispersed on the ceria surface like small clusters that cannot be detected by XRD [25–27]. These results show the crystalline ceria formation both by hydrothermal or precipitation method. The crystallite of ceria on CeO_2-HT and CeO_2-PP supports has its average size estimated respectively in 9.3 and 10.6 nm (Table 1) from the peak broadening using Scherrer's equation. In CuO/CeO_2-HT and CuO/CeO_2-PP catalysts, the ceria average particle sizes have been 9.2 and 9.7 nm respectively. Therefore, it is possible to observe that both catalysts presents small ceria crystallites. Also, the addition of CuO in ceria lattice led to a smaller crystallite size compared to the results of supports and their respective catalysts. This is probably due the redispersion of CeO_2 particles motivated by the presence of Cu species during the preparation conditions. According to Amin et al., in a catalyst with low copper content all lattice vacancies of ceria support are accessible to Cu^{+2} ions and subsequently form a highly dispersed layer of Cu species with exhibited high metal-support interaction. This observation is very important for the catalytic activity in PROX-CO reaction, due to the fact that smaller particles provide more structural defects, which is beneficial to oxidation reaction [28,29].

Fig. 4 shows the TEM micrographs of CuO/CeO_2-HT and CuO/CeO_2-PP catalysts. The average CuO particle size is around 2 nm

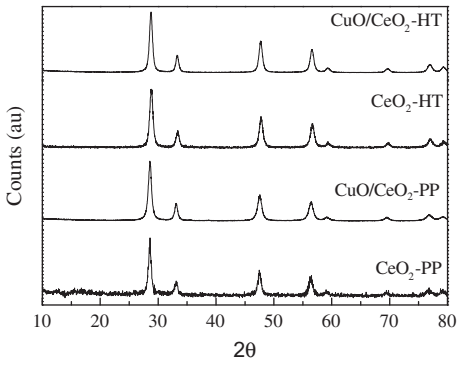

Fig. 3. XRD patterns of CeO_2-HT, CeO_2-PP and CuO/CeO_2 catalysts.

Table 1
Textural properties of CeO_2-HT, CeO_2-PP and CuO/CeO_2 catalysts.

Sample	Average ceria crystallite size (nm)	Surface area ($m^2\ g^{-1}$)
CeO_2-HT	9.3	72
CeO_2-PP	11	44
CuO/CeO_2-HT	9.2	63
CuO/CeO_2-PP	9.7	34

in CuO/CeO_2-HT and 3 nm in CuO/CeO_2-PP and these values are consistent if compared with those observed by other characterization techniques. The metal particle size is fundamental for improving performance in PROX-CO oxidation; smaller metal particles favor both CO conversion and selectivity. According to Liu et al., Cu can interact with CeO_2 through several possible forms: CuO clusters, bulk CuO and solid solution of CuO and CeO_2 (not observed in these samples by XRD analysis). Due to the low atomic weight of copper and the poor contrast, CuO particles cannot be distinguished from cerium even in the resolution of electron microscopy image. Gomez-Cortes et al. showed that some evidence of CuO crystal was obtained only in samples with high copper content. Furthermore, the selected area electron diffraction (SAED) patterns in Fig. 4 indicated that both samples were crystalline in local areas [12,20,21,30,31].

Fig. 5 shows the photomicrography of the calcined catalysts. Results reveal that the CuO/CeO_2-HT presents a well defined plaque shape structure, while CuO/CeO_2-PP have a spongy aspect one. Complementing the SEM/FEG analysis, an EDX mapping sweep was made and the micrographs are shown in Fig. 6: it is possible to observe a homogeneous distribution of Cu on the CuO/CeO_2-HT catalyst, while on the CuO/CeO_2-PP the Cu is concentrated in specific regions on the surface, representing a strong clue for a better dispersion of CuO in the first sample, in agreement with the H_2-TPR, BET surface area and XRD analysis.

Textural and chemical analysis results obtained by BET and XPS are reported in Tables 1 and 2 respectively and SEM Atomic Scanning results are presented in Fig. 6. As shown in the Table 1, the specific surface area of CuO/CeO_2-HT is higher than CuO/CeO_2-PP, as well as the BET area of CeO_2-HT is greater than CeO_2-PP. This shows that the hydrothermal method of support preparation resulted in a solid with smaller particle size when compared with the samples synthesized by the conventional precipitation. According to Zec et al., ceria with crystallites size into nanometer range enhances redox capability and ionic conductivity of CeO_2 due to its higher mobility, primarily of the oxygen ions [5]. Thus, the catalyst supported on CeO_2-HT has a higher specific surface area and a consequent greater dispersion than the CuO/CeO_2-PP. It is noteworthy that the greater dispersion of the metal on ceria favors the catalytic activity and the selectivity of PROX-CO reaction. Also, a crystal size decreasing with copper addition might imply that copper atoms, of smaller size than cerium atoms, are being incorporated into the ceria lattice [32,33]. Thus, particles of the solids prepared by hydrothermal method are smaller, therefore can be considered of larger surface area. Also, bulk elemental analysis of the CuO/CeO_2-PP and CuO/CeO_2-HT (Table 2) reveals that the deposition–precipitation route is appropriated for the preparation of those catalysts, as other characterization results have shown previously. However, XPS measurements show that CuO/CeO_2-HT catalyst has a significant copper surface coating compared to CuO/CeO_2-PP, indicating that this CuO is more homogeneously

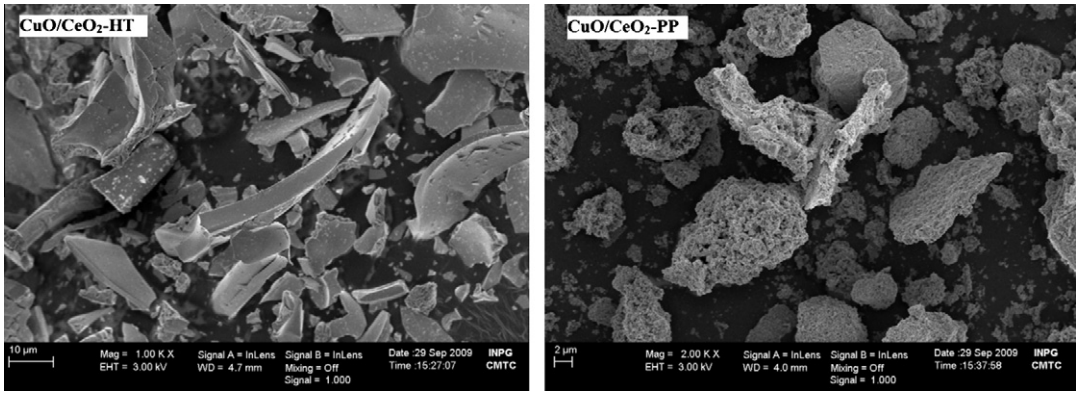

Fig. 4. TEM images of CuO/CeO_2-HT and CuO/CeO_2-PP.

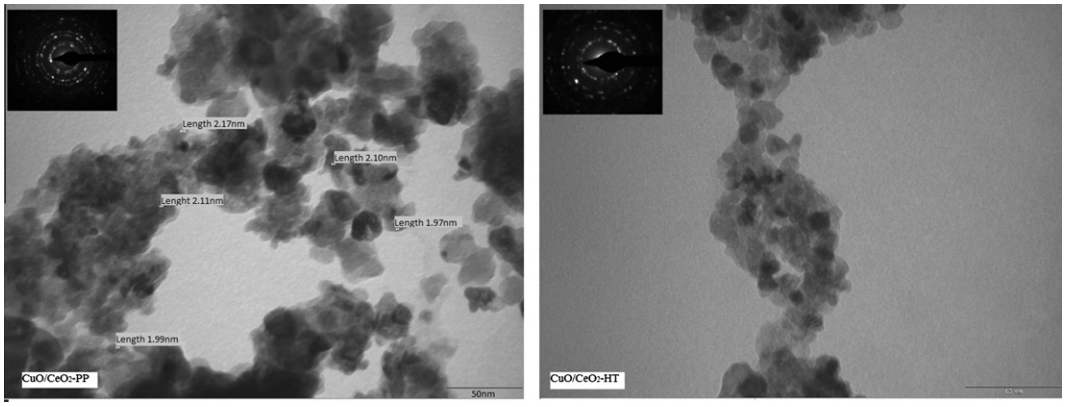

Fig. 5. FEGSEM characterization of CuO/CeO_2-HT and CuO/CeO_2-PP.

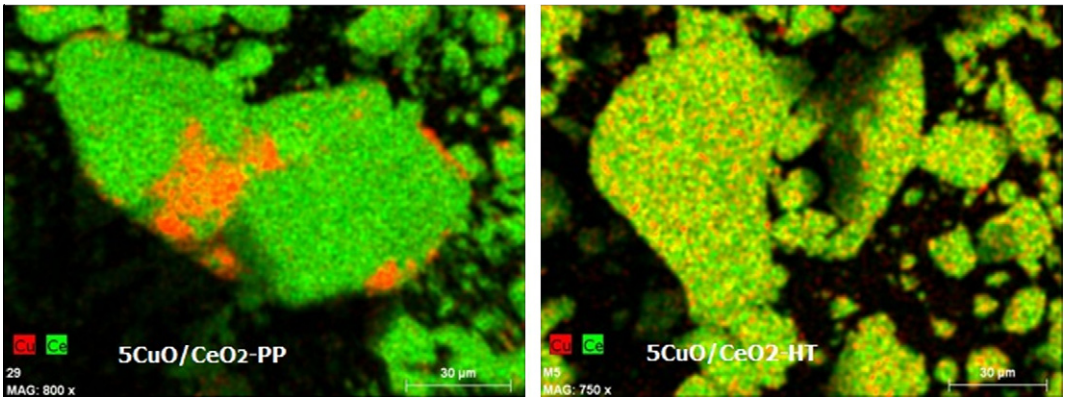

Fig. 6. SEM Atomic Scanning of CuO/CeO_2-HT and CuO/CeO_2-PP catalysts.

Table 2
Bulk and surface chemical compositions of CuO/CeO_2 catalysts.

Catalysts	Bulk composition (wt%)[a]				Surface composition (wt%)[b]			
	Ce	Cu	O	Ce:Cu	Ce	Cu	O	Ce:Cu
CuO/CeO_2-HT	75	4.0	21	19	68	3.9	28	17
CuO/CeO_2-PP	76	3.6	20	21	65	3.1	32	21

[a] Determined by atomic absorption.
[b] Determined by XPS.

dispersed on CeO_2-HT support, as also showed by SEM/EDX analysis. Fig. 6 clearly demonstrates it, where pictures show that Cu is dispersed on all ceria surfaces, while on CuO/CeO_2-PP the CuO is concentrated in a few parts of the support. The morphological characteristics such as greater surface area and smooth structure in the form of plaques with smaller ceria crystallite size presented by the ceria-HT promotes the dispersion of small particles of copper over the entire surface of ceria, as observed for the CuO/CeO_2-HT catalyst. The CuO/CeO_2-PP catalyst has spongy structure with large crystals and low specific surface area, in which CuO is present as isolated points on ceria's surface resulting in the lowest provision of active sites per area.

Figs. 7 and 8 show the activity and selectivity curves in the CO preferential oxidation reaction conditions. Both catalysts are active and there is a high optimum temperature for CO conversion, i.e. there is a temperature in which the conversion of CO to CO_2 is maximum. At 150 °C, CuO/CeO_2-PP catalyst presents about 95% of conversion and at 100 °C this conversion is not higher than 70%. The CuO/CeO_2-HT catalyst behavior is better than the CuO/CeO_2-PP, especially at low temperatures. The conversion rate of this catalyst, above 200 °C, increased in about 80%; with CuO/CeO_2-PP catalyst the conversion showed continuous decrease at temperatures higher than 150 °C, getting 50% at 300 °C. As for the first catalyst, the activity increases as the temperature decreases, disregarding the atypical behavior at 200 °C. At 150 °C, the activity is near 100% and keeps it even at 100 °C, showing that this catalyst is efficient at low temperatures. The behavior of these catalysts may be associated to the particle sizes and different

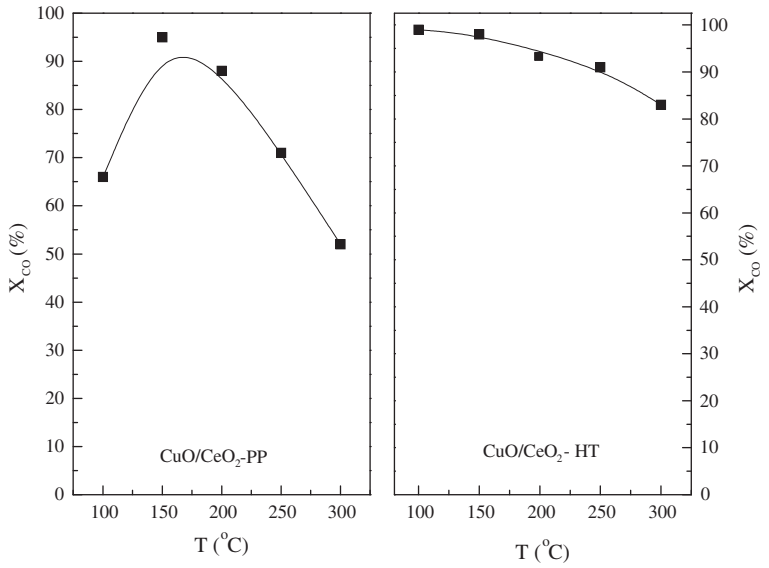

Fig. 7. CO conversion versus temperature for CuO/CeO_2-HT and CuO/CeO_2-PP catalysts. Reaction conditions: 50%H_2, 4%CO, 2%O_2, N_2.

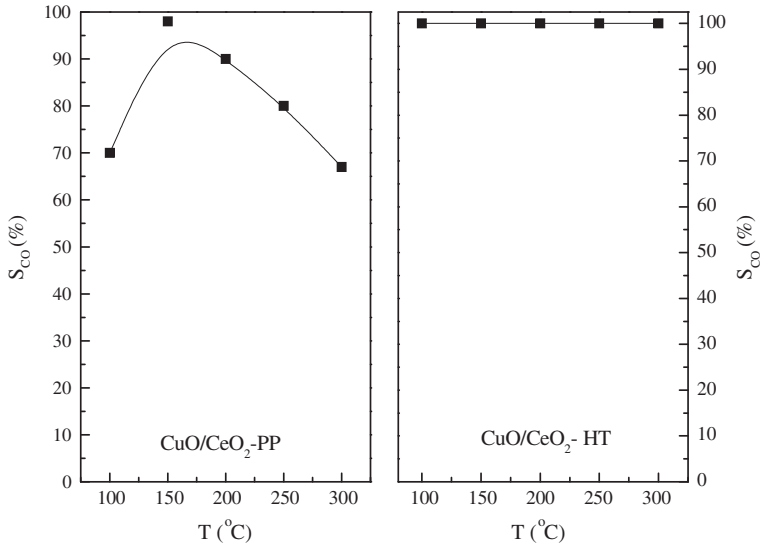

Fig. 8. Selectivity versus temperature for CuO/CeO_2-HT and CuO/CeO_2-PP catalysts. Reaction conditions: 50%H_2, 4%CO, 2%O_2, N_2.

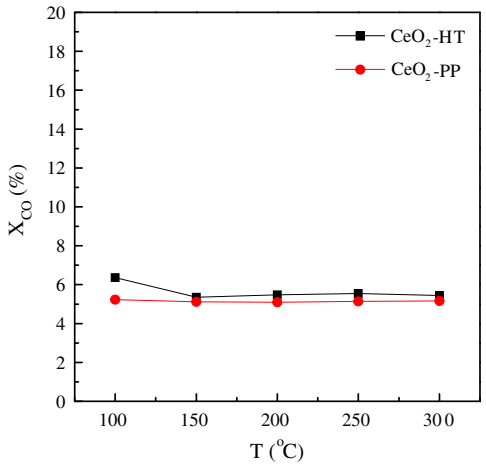

Fig. 9. CO conversion versus temperature for CeO_2-HT and CeO_2-PP. Reaction conditions: 50%H_2, 4%CO, 2%O_2, N_2.

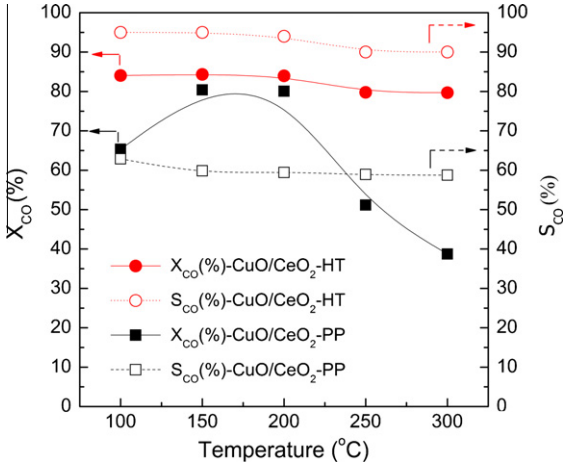

Fig. 10. CO conversion versus temperature for CuO/CeO_2-HT and CuO/CeO_2-PP. Reaction conditions: 50%H_2, 4%CO, 2%O_2, 10% CO_2, 15%H_2O, N_2.

dispersion degrees, like observed by the applied characterization techniques. The supports preparation method showed a relevant influence on the catalysts final features and, through the applied techniques, there was a clear performance improvement for CuO/CeO_2-HT catalyst, confirmed by the catalytic activity test. This catalyst also presents a higher selectivity in PROX reaction, as shown in Fig. 8. The CuO/CeO_2-HT catalyst did not promote the H_2 to H_2O oxidation and the CO_2 selectivity was constant and equal to 100% during all the temperature range. It is known that the reaction occurs through a redox cycle, most likely between CuO and Cu_2O. The active sites are generally assumed to be fine copper or copper oxide clusters highly dispersed on CeO_2 support [33]. Also, according to Liu et al., oxygen species on an oxide catalyst include various types of adsorbed oxygen and lattice oxygen. In general, the former is considered important for complete oxidation or combustion, while the latter contributes to selective oxidation [34]. This may explain the best selectivity of the CuO/CeO_2-HT catalyst, although in terms of catalytic activity both showed interesting results.

This way, besides being more active, the CuO/CeO_2-HT catalyst features favored the CO oxidation reaction instead of water formation reaction, an important fact for the hydrogen purification application on PEMFC cells. Is also important to note that, in terms of the temperature at which it shows higher activity, the CuO/CeO_2-HT catalyst is also more appropriate to fuel cells operating at low temperatures.

Comparing the performance of CuO/CeO_2 series catalysts with some systems in the literature, it could be observed that the copper-ceria catalyst may be attempted since the system shows catalytic activity similar to traditional noble metal catalysts. Pozdnyakova et al. showed that 1%Pt/CeO_2 catalyst had presented XCO = 0.90 and SCO = 0.50 at 100 °C [35]. Teschner et al. showed that PtSn supported catalyst presented the best result of XCO = 0.4 and SCO = 0.55 at 100 °C [36]. Laguna et al. had prepared gold-containing catalysts supported in Ce–Zr, Zn and Fe mixed oxides for PROX-CO reaction. At 100 °C, the best performance showed around XCO = 0.75 and the reverse water gas shift reaction was associated with the PROX-CO reaction [37]. Ilieva et al. also studied gold catalyst (Au/CeO_2 doped with Fe_2O_3 and MnO_2) and proved that the catalytic activity was satisfactory for the PROX-CO reaction with all catalysts, showing the best result of XCO = 1.00 at 100 °C. However, at this temperature the selectivity was found around 0.40 [38].

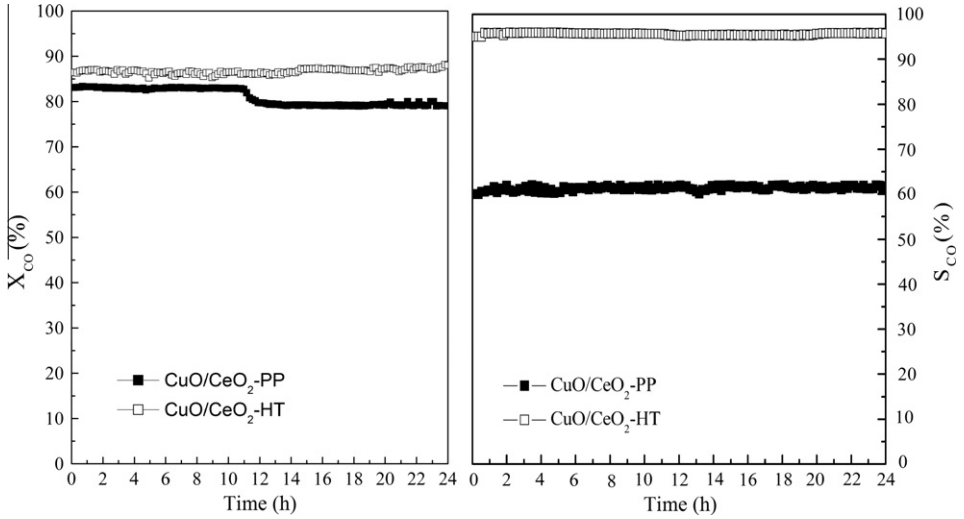

Fig. 11. Long-term reaction for real PROX-CO reaction. Reaction conditions: 50%H_2, 4%CO, 2%O_2, 15% CO_2, 10%H_2O, N_2. Temperature: 150 °C.

Fig. 9 presents the catalytic activity obtained with the CeO_2-HT and CeO_2-PP supports. The results showed that the nature of ceria does not influence the catalytic activity and selectivity, and both supports have the same profile: small conversion of CO to CO_2 at all reaction temperatures and selectivity for CO_2 formation of 100%. These results explain the importance of the strong interaction existent between ceria and copper, and that a small CuO content is sufficient to enhance the catalytic activity. The nature of ceria is important in catalytic activity on the system CuO/CeO_2, where other factors like particle size, dispersion, morphology and thermal stability influence the catalysts properties and consequently the activity.

The effect of CO_2 and H_2O addition in the reactor feed stream was studied in the test called real PROX-CO reaction. The result of catalytic activity is presented in Fig. 10. The presence of CO_2 and H_2O affect the CO conversion for both catalysts. The profile of CO conversion is similar to reaction with absence of CO_2 and H_2O: the CuO/CeO_2-HT presents best performance than CuO/CeO_2-PP catalyst in all temperature tested, indicating that catalyst prepared by hydrothermal method is more tolerant to CO_2 and H_2O. It is possible to observe also that CO conversion decreases in both catalyst compared with ideal PROX-CO reaction: XCO = 84% for CuO/CeO_2-HT and 80% for CuO/CeO_2-PP catalysts at 150 °C in the real PROX-CO reaction. The reaction's selectivity has similar behavior and the addition of CO_2 and H_2O provokes a decrease in SCO values for both catalysts. However, the CuO/CeO_2-HT showed the best result, with SCO around 95%. Similar results were described in the literature for CuO–CeO_2 system and the decrease of catalytic activity can be attributed to the competitive adsorption of the CO_2 and the blockage of active sites by H_2O molecules, inhibiting the CO conversion [12,31,39–41].

Long-term stability tests at 150 °C were presented in Fig. 11. The catalysts were tested for 24 h in presence of CO_2 and H_2O. The result reveals that CuO/CeO_2-HT presented no deactivation in 24 h, maintaining the CO conversion around 85% and selectivity around 95%. Although CuO/CeO_2-PP also showed good results for CO conversion (around 82%), it is possible to observe that after 10 h of real PROX-CO reaction the activity was 80%. This indicates a small decrease in that catalyst's activity, however the selectivity remained constant and equal 60% in all 24 h. These results are a further indication that the CuO/CeO_2-HT catalyst has the most favorable characteristics for PROX-CO when compared to CuO/CeO_2-PP, as observed along the text.

4. Conclusions

The nature of ceria influences the catalytic activity of the CuO/CeO_2 catalyst, but the activity of both CeO_2-PP and CeO_2-HT supports is similar, showing the importance of metal-support interaction for the PROX-CO reaction. Thus, CeO_2-HT had a larger surface area and smaller crystallite size than CeO_2-PP and the catalyst CuO/CeO_2-HT was the best for PROX-CO reaction. Its higher activity and selectivity were attributed to a combination of different properties: (i) the morphology and the small crystallite size of CeO_2-HT favors the catalyst with largest surface area, and as a consequence, there is better dispersion of these small CuO particles in ceria; (ii) the small crystallites size of ceria enhances redox capability and ionic conductivity of CeO_2 due to the higher mobility, primarily of the oxygen ions, important for PROX-CO mechanism; (iii) this catalyst has copper species that reduce at low temperature and are more reactive than copper at small dispersion state. This catalyst has shown the same profile of conversion and selectivity along all experiment. The long-term stability test and the effect of CO_2 and H_2O addition in feed gas showed that CuO/CeO_2-HT is stable for 24 h and more tolerant to carbon dioxide and water than CuO/CeO_2-PP.

Acknowledgements

The authors are grateful to Brazilian agencies Capes, CNPq and FAPESP for grants and financial support.

References

[1] Qian K, Lv S, Xiao X, Sun H, Lu J, Luo M, et al. J Mol Catal A: Chem 2009;306:40.
[2] Ozawaa M, Loong C. Catal Today 1999;50:329.
[3] Jiang X, Lu G, Zhou R, Mao J, Chen Y, Zheng X. Appl Surf Sci 2001;173:208.
[4] Huang S, Li L, Van der Biest O, Vleugels J. Solid State Sci 2005;7:539.
[5] Zec S, Boskovic S, Kaluperovic B, Bogdanov Z, Popovic N. Ceram Int 2009;35:195.
[6] Yee A, Morrison SJ, Idriss H. Catal Today 2000;63:327.
[7] Wootsch A, Descorme C, Duprez D. J Catal 2004;225:259.
[8] Martınez-Arias A, Fernandez-Garcıa M, Soria J, Conesa JC. J Catal 1999;182:367.
[9] Marino F, Descormea C, Duprez D. Appl Catal B 2005;58.
[10] Manzoli M, Di Monte R, Boccuzzi F, Coluccia S, Kaspar J. Appl Catal B 2005;61.
[11] Zhou K, Xu R, Sun X, Chen H, Tian Q, Shen D, et al. Catal Lett 2005;101:169.
[12] Peng C, Lia H, Liaw B, Chen Y. Chem Eng J 2011;172:452.
[13] Mai H, Mengfei L, Ping F. J Rare Earths 2006;24:188–92.
[14] Luo M, Zhong Y, Yuan X, Zheng X. Appl Catal A 1997;162.
[15] Xiaoyuan J, Guanglie L, Renxian Z, Jianxin M, Yu C, Xiaoming Z. Appl Surf Sci 2001;173.

[16] Li L, Song L, Wang H, Chen C, She Y, Zhan Y, et al. Int J Hydrogen Energy 2011;36:8839.
[17] Dong X, Zou H, Lin W. Int J Hydrogen Energy 2010;31:2337.
[18] Guo X, Mao D, Lu G, Wang S, Wu G. J Catal 2010;271:178.
[19] Gu C, Lu S, Miao J, Liu Y, Wang Y. Int J Hydrogen Energy 2010;35:6113.
[20] Zheng X, Zhang X, Wang X, Wang S, Wu S. Appl Catal A 2005;295.
[21] Zheng X, Zhang X, Wang S, Wang X, Wu X. J Nat Gas Chem 2007;16:179.
[22] Cui MY, Yao XQ, Dong WJ, Tsukamoto K, Li CR. J Cryst Growth 2010;312:287.
[23] Wang S, Xu H, Qian L, Jia X, Wang J, Liu Y, et al. J Solid State Chem 2009;182:1088.
[24] Chen L, Li L, Li G. J Alloys Compd 2008;464:532.
[25] Hu C, Zhu Q, Jiang Z, Zhang Y, Wang Y. Micropor Mesopor Mater 2008;113:427.
[26] Fox E, Velua S, Engelhard MH, Chin YH, Miller JT, Kropf J. J Catal 2008;260:358.
[27] Pérez-Hernández R, Gutiérrez-Martínez A, Gutiérrez-Wing CE. Int J Hydrogen Energy 2007;32:2888.
[28] Amin NAS, Tan EF, Manan ZA. Appl Catal B 2003;43.
[29] Guo MN, Guo CX, Jin LY, Wang YJ, Lu JQ, F Luo M. Mater Lett 2010;64:1638.
[30] Liu Z, Zhou R, Zheng X. J Nat Gas Chem 2008;17:125.
[31] Gómez-Córtes A, Márquez Y, Arenas-Alatorre J, Diaz G. Catal Today 2008;133–135:743.
[32] Marban G, Fuertes AB. Appl Catal B 2005;57.
[33] Zhang WJ, Dey SP, Deevi S. Appl Catal A 2005.
[34] Liu W, Flytzani-Stephanopoulos M. Chem Eng J 1996;64:283.
[35] Pozdnyakova O, Teschner D, Wootsch A, Krohnert J, Steinhauer B, Sauer H, et al. J Catal 2006;237:1.
[36] Teschner D, Wootsch A, Paal Z. Appl Catal A: Gen 2012;411:31.
[37] Laguna OH, Sarria FR, Centeno MA, Odriozola JA. J Catal 2010;276:360.
[38] Ilieva L, Panaleo G, Ivanov I, Zanella R, Sobczak JW, Lisowski W, et al. Catal Today 2011;175:411.
[39] Ayastuy JL, Gamboa NK, González-Marcos MP, Gutierrez-Ortiz MA. Chem Eng J 2011;171:224.
[40] Liu Z, Zhou R, Zheng X. Int J Hydrogen Energy 2008;33:791.
[41] Valdés-Solís T, López I, Marbán G. Int J Hydrogen Energy 2010;35:1879.